Asian Journal of Chemistry; Vol. 38, No. 7 (2026), 1843-1852
ASIAN JOURNAL OF CHEMISTRY
https://doi.org/10.14233/ajchem.2026.35855

Synthesis and Characterisation of Marine Docosahexaenoic Acid-Encapsulated Chitosan Nanoparticles (DHA@CSNP) and Evaluation of their Antioxidant and Cytotoxic Activities

JENI VIJAYAKUMAR and MIRUNALINI SANKARAN*,

Department of Biochemistry and Biotechnology, Annamalai University, Annamalainagar-608002, India

*Corresponding author: E-mail: mirunasankar@gmail.com

Received: 5 March 2026 *Accepted*: 8 June 2026 *Published online*: 3 July 2026 AJC-22410

Docosahexaenoic acid (DHA) is an essential ω-3 polyunsaturated fatty acid with demonstrated health benefits, including neuroprotection, anti-inflammatory effects and anticancer activity. However, its poor water solubility, susceptibility to oxidative degradation and low bioavailability limit therapeutic applications. This study aimed to improve the stability and therapeutic efficacy of DHA through nano-encapsulation within chitosan nanoparticles (DHA@CSNPs), synthesised through ionic gelation method using sodium tripolyphosphate as a crosslinking agent. The synthesised nanoparticles were characterised by SEM, FE-SEM with EDX, FTIR, XRD, DLS and zeta potential analysis. DHA@CSNPs exhibited nanoscale morphology (average particle size 76.53 ± 3.41 nm), semi-crystalline structure and a positive surface charge of 21.63 mV, confirming colloidal stability and successful encapsulation. Encapsulation efficiency was 83.38 ± 1.48% and *in vitro* release studies demonstrated pH-dependent sustained release, with higher release at acidic pH, mimicking tumor microenvironments. Antioxidant potential was evaluated using ABTS, DPPH, hydroxyl, superoxide, nitric oxide and reducing power assays, showing enhanced radical-scavenging activity and lower IC_{50} values for DHA@CSNPs than for free DHA. Cytotoxicity against MDA-MB-231 triple-negative breast cancer cells revealed a dose-dependent decrease in cell viability with an IC_{50} of 59.30 µg/mL and pronounced morphological changes indicative of apoptosis. These results highlight that chitosan-based nanocarriers effectively improve DHA's stability, bioavailability and therapeutic potential.

Keywords: Docosahexaenoic acid, Chitosan nanoparticles, Ionic gelation, Nanoencapsulation, Antioxidant activity, Breast cancer.

INTRODUCTION

Docosahexaenoic acid (DHA) is a long-chain omega-3 polyunsaturated fatty acid (ω-3 PUFA) containing 22 carbon atoms and is mainly obtained from marine fish, such as salmon, tuna and fish oils [1,2]. DHA is an important component of cell membranes and plays a key role in lipid metabolism, neural development, vision, and the regulation of inflammatory responses [3,4]. DHA deficiency has been associated with several disorders, including cancer, atherosclerosis, fatty liver disease and inflammatory gastrointestinal diseases [5-8]. Adequate DHA intake has been reported to reduce the risk or severity of cardiovascular disease, asthma, depression, attention deficit hyperactivity disorder, rheumatoid arthritis, and other autoimmune conditions [9]. As a major constituent of the brain and retina, DHA is essential for normal cognitive function, nerve development, and visual health, making it important for maintaining overall human health [10].

Although DHA can be synthesised in the human body from α-linolenic acid (ALA), which is abundant in certain plant oils such as flaxseed and perilla oil, through the action of fatty acid elongates and desaturases, the conversion efficiency is extremely low. The bioconversion rate in humans generally ranges from 2% to 10% and in some cases has been reported as low as 0.01% [11,12]. Therefore, DHA-rich or fortified foods and DHA supplements are the two main exogenous sources to obtain additional DHA needed for the biological functions of the human body. However, DHA cannot be synthesised de novo in sufficient quantities in the human body and must therefore be obtained from dietary sources or through limited conversion of α-linolenic acid (ALA) [13]. Owing to its highly unsaturated structure, DHA is susceptible to the oxidative degradation and exhibits poor aqueous solubility, which can reduce its stability and bioavailability and restrict its pharmaceutical application [13-15].

Nano-encapsulation offers a promising strategy to overcome these limitations by protecting DHA from degradation and improving its delivery to target sites [16,17]. Among various nanocarriers, chitosan has received considerable attention due to its biocompatibility, biodegradability, low toxicity and mucoadhesive nature. Its cationic surface facilitates interaction with biological membranes, enhances cellular uptake, improves the bioavailability of poorly soluble compounds, and enables controlled drug release [18,19]. Since oxidative stress, caused by excessive production of reactive oxygen species (ROS), contributes to cellular damage and disease progression, the antioxidant properties of DHA-loaded nanoparticles are of particular interest [20-24].

In this study, DHA-loaded chitosan nanoparticles (DHA@CSNPs) were prepared using the ionic gelation method. The nanoparticles were characterised using SEM, FE-SEM/EDX, DLS, zeta potential, FTIR and XRD techniques. Encapsulation efficiency, pH-responsive drug release, antioxidant activity and cytotoxicity against MDA-MB-231 breast cancer cells were evaluated to assess their potential as a nanodelivery system.

EXPERIMENTAL

Docosahexaenoic acid, chitosan (low molecular weight, degree of deacetylation 75-85%) and sodium tripolyphosphate (TPP) were sourced from Sigma-Aldrich, USA. Azino-*bis*(3-ethylbenzothiazoline-6-sulfonic acid) (ABTS), 1,1-diphenyl-2-picrylhydrazyl radical (DPPH), nitro blue tetrazolium (NBT), ferric chloride, potassium persulphate, trichloroacetic acid (TCA), nicotinamide adenine dinucleotide (NADH), phenazine methosulphate (PMS), thiobarbituric acid (TBA), ethylenediaminetetraacetic acid (EDTA), 2-deoxyribose, hydrogen peroxide, ethanol, phosphate-buffered saline (PBS), ascorbic acid and were also obtained from Sigma-Aldrich (USA). Mostly all chemicals used were of analytical grade and ultra-pure water was used to prepare all stock solutions.

Synthesis of docosahexaenoic acid-loaded chitosan nanoparticles (DHA@CSNPs): DHA@CS-NP was synthesised by the ionic gelation method using TPP as a gelating agent [25]. The synthesis of chitosan nanoparticles was initially optimised by varying the concentrations of chitosan and TPP. Chitosan was dissolved in 1% (v/v) acetic acid and stirred overnight at room temperature to obtain a homogeneous solution. The pH was adjusted to 5.0 using 1 M NaOH. Subsequently, 100 mg of DHA dissolved in 0.5% (v/v) DMSO was added to the freshly prepared chitosan solution and stirred for 1 h to ensure uniform dispersion. Thereafter, an equal volume of TPP solution (1 mg mL^{-1}) was added dropwise under continuous mild stirring. The mixture was further stirred for 1 h, allowing ionic crosslinking between chitosan and TPP, resulting in the formation of DHA-encapsulated chitosan nanoparticles (DHA@CSNPs). The entire process was carried out at room temperature. The synthesised nanoparticles were separated by centrifugation and the resulting pellets were collected, freeze-dried and stored at 4 °C until further characterization.

Characterisation: The optical properties of DHA@CSNPs were examined using a UV-Vis spectrophotometer (Analytik Jena, Germany) over the wavelength range of 200-800 nm. Fourier transform infrared (FTIR) spectra were recorded on a Shimadzu FTIR 8201-PC spectrophotometer within the range of 4000-400 cm^{-1} using the KBr pellet to identify functional groups and investigate the interactions between DHA and chitosan. The morphology and surface characteristics of the nanoparticles were analysed using scanning electron microscopy (SEM) and field-emission scanning electron microscopy (FE-SEM). Prior to imaging, samples were sputter-coated with a thin layer of gold to improve conductivity. Elemental composition was determined using energy-dispersive X-ray (EDX) spectroscopy coupled with the FE-SEM system. The hydrodynamic particle size, polydispersity index (PDI) and zeta potential of DHA@CSNPs were measured by dynamic light scattering (DLS) using a Nano-ZS ZEN 3600 instrument (Malvern Instruments Ltd., U.K.) at 25 ºC. The crystalline structure of the nanoparticles was investigated using X-ray diffraction (XRD) analysis on a Bruker D2 Phaser diffractometer employing CuKα radiation (λ = 1.5406 Å). Diffraction patterns were recorded over a 2θ range of 10-80º at room temperature.

Encapsulation efficiency (EE): The DHA@CSNP suspension was centrifuged at 13,000 rpm for 20 min. The supernatant was collected and the free DHA level was measured by a UV-vis spectrophotometer (Shimadzu, Japan) at a wavelength of 390 nm [26]. The encapsulation efficiency was calculated using eqn. 1:

$$\text{Encapsulation efficiency (\%)} = \frac{A - B}{A} \times 100 \quad (1)$$

where A = total drug initially used; and B = unencapsulated drug quantity.

***In vitro* drug release:** The release profile of DHA from CSNPs was studied under physiological (pH 7.4) and acidic (pH 5.4) conditions. Nanoparticle suspensions were placed in dialysis bags and immersed in PBS) at 37 ºC with gentle stirring [27]. At predetermined time intervals, aliquots were withdrawn and analysed spectrophotometrically to determine the cumulative drug release percentage.

ABTS radical cation decolourisation assay: The ABTS radical cation decolourisation assay was used to assess the total antioxidant capacity of DHA. The ABTS radical cation was generated by reacting 7 mM ABTS with 2.5 mM $K_2S_2O_8$ and incubating the mixture in the dark at room temperature for 12-16 h, producing a stable blue-green chromophore. Different concentrations of DHA (10-50 μg/mL) were added to 2.7 mL of ABTS solution to obtain a final volume of 3 mL and the mixture was incubated for 30 min [28]. Absorbance was measured at 734 nm. Ascorbic acid served as the standard and scavenging activity was calculated relative to the control.

The percentage of radical scavenging activity was calculated using the following formula:

$$\text{Scavenging (\%)} = \frac{\text{Control OD} - \text{Test OD}}{\text{Control OD}} \times 100$$

DPPH radical scavenging assay: The DPPH radical scavenging assay was used to evaluate the antioxidant activity of DHA. Different concentrations of DHA (10-50 μg/mL) were mixed with 1 mL of 0.5 mM DPPH solution in ethanol and 2 mL of 0.1 M acetate buffer (pH 5.5). After

incubation for 30 min in the dark at room temperature, absorbance was measured at 517 nm [29]. Ascorbic acid served as the standard and reduced absorbance indicated greater radical-scavenging activity.

$$\text{Scavenging (\%)} = \frac{\text{Control OD} - \text{Test OD}}{\text{Control OD}} \times 100$$

Hydroxyl radical scavenging assay: In this method, hydroxyl radicals are generated through the reduction of H_2O_2 by transition metal ions in the presence of ascorbic acid. These radicals degrade deoxyribose into products that form a pink chromogen upon heating with TBA. DHA inhibits colour development by competing with deoxyribose for hydroxyl radicals. The reaction mixture (1 mL) contained phosphate buffer, varying concentrations of DHA (10-50 µg/mL), $FeCl_3$, EDTA, ascorbic acid, H_2O_2 and 2-deoxyribose. After incubation for 60 min at room temperature, TBA and TCA were added and the mixture was heated for 30 min [30]. The absorbance was measured at 535 nm. Ascorbic acid was used as the positive control and a decrease in absorbance was taken as an indication of hydroxyl radical scavenging activity. The following formula was used to calculate radical scavenging:

$$\text{Scavenging (\%)} = \frac{\text{Control OD} - \text{Test OD}}{\text{Control OD}} \times 100$$

Superoxide anion radical scavenging assay: The superoxide anion radical scavenging activity was determined using the nitro blue tetrazolium (NBT) reduction assay [31]. Superoxide anion scavenging activity was evaluated using the PMS-NADH-NBT system. In this assay, superoxide radicals generated by the PMS-NADH coupling reaction reduce NBT to form a violet-coloured formazan product, which was measured at 560 nm. Different concentrations of DHA (10-50 µg mL^{-1}) were mixed with NBT and NADH solutions, and the reaction was initiated by the addition of PMS. After incubation at 30 ºC for 15 min, the absorbance was recorded at 560 nm. Ascorbic acid was used as the positive control, while a reagent blank containing distilled water served as negative control. A decrease in absorbance indicated superoxide radical scavenging activity. A decrease in absorbance reflected enhanced superoxide anion scavenging activity.

$$\text{Scavenging (\%)} = \frac{\text{Control OD} - \text{Test OD}}{\text{Control OD}} \times 100$$

Reducing sugar assay: The reducing power was evaluated using the potassium ferricyanide reduction method [32]. A 1.0 mL of different concentrations of DHA (0.47-6.0 mg mL^{-1}) in phosphate buffer (0.2 M, pH 6.6) was dissolved in 1.0 mL of potassium ferricyanide (1%, w/v) and incubated at 50 ºC for 20 min. The reaction was then terminated by adding 2.0 mL of trichloroacetic acid (10% w/v) to the mixture. The solution was then mixed with 1.2 mL of $FeCl_3$ (0.1% w/v) and the absorbance was measured at 700 nm. Increased absorbance of the reaction mixture indicated an increasingly reducing power.

Nitric oxide (NO) radical scavenging assay: The NO radical scavenging activity was determined using the sodium nitroprusside Griess reaction method [33]. Sodium nitroprusside (5 mM) in phosphate-buffered saline (pH 7.3) was incubated with various concentrations of DHA for 180 min at 25 ºC using a 25 W tungsten lamp as visible light source. During incubation, sodium nitroprusside generated nitric oxide, which reacted with oxygen to form nitrite ions. At 30 min intervals, aliquots of the reaction mixture were treated with Griess reagent containing sulphanilamide and naphthyl ethylenediamine dihydrochloride. The resulting azo dye was quantified by measuring absorbance at 546 nm. Nitrite concentration was determined from a calibration curve prepared using standard sodium nitrite solutions.

Cytotoxicity assay: MDA-MB-231 cells were seeded in 96-well plates at a density of 1×10^4 cells/well in 100 µL of complete DMEM medium and incubated at 37 ºC with 5% CO_2 for 24 h. After adherence, cells were treated with DHA @CSNPs at concentrations of 5, 10, 20, 40, 80, 160 and 320 µg/mL in a final volume of 100 µL per well and incubated for an additional 24 h. Cell viability was assessed using the MTT assay by adding 10 µL of 5 mg/mL MTT solution to each well, followed by incubation for 3 h at 37 ºC. The formed formazan crystals were dissolved in 100 µL of DMSO and the absorbance was measured at 570 nm using a microplate reader. Morphological changes were observed under a phase-contrast microscope at 100× magnification to detect hallmarks of apoptosis, including cell shrinkage, rounding, membrane blebbing and cytoplasmic vacuolisation, while untreated control cells were maintained under identical conditions.

Statistical analysis: All experimental data were presented as the mean ± standard deviation (SD) of three independent experiments (n = 3). Statistical differences between groups were analysed using one-way analysis of variance (ANOVA) followed by Tukey's post hoc test. Differences were considered statistically significant at $p < 0.05$, highly significant at $p < 0.01$ and very highly significant at $p < 0.001$.

RESULTS AND DISCUSSION

UV-visible spectroscopy: Fig. 1 shows the UV-visible spectra of pure DHA, CNPs and DHA@CSNPs. Pure DHA exhibited a prominent absorption maximum at 316 nm, indicative of its intrinsic electronic transitions. In contrast, pure chitosan displayed an absorption peak at 260 nm, corresponding to the n→π* transitions of its functional groups. The DHA@CSNPs showed a shifted absorption peak at 288 nm, suggesting successful encapsulation of DHA within the chitosan matrix and possible interactions between DHA and the polymer backbone. This red shift in the absorption peak of the nanoparticles, compared to pure chitosan and DHA, indicates the formation of a stable nanoparticulate system with altered electronic environments. The absorption peak observed for DHA@CSNPs is consistent with previously reported values for chitosan nanoparticles, which typically exhibit characteristic bands in the 200-342 nm region [34-37]. The agreement with earlier studies confirms the successful formation of DHA@CSNPs and supports their subsequent structural and functional characterization.

FTIR studies: Fig. 2 illustrates the FTIR spectra of CNPs (a), DHA (b) and DHA@CSNPs (c). The spectrum of CNPs displayed characteristic peaks at 3286.14 cm^{-1} corresponding to N–H and O–H stretching vibrations of amine and hydroxyl

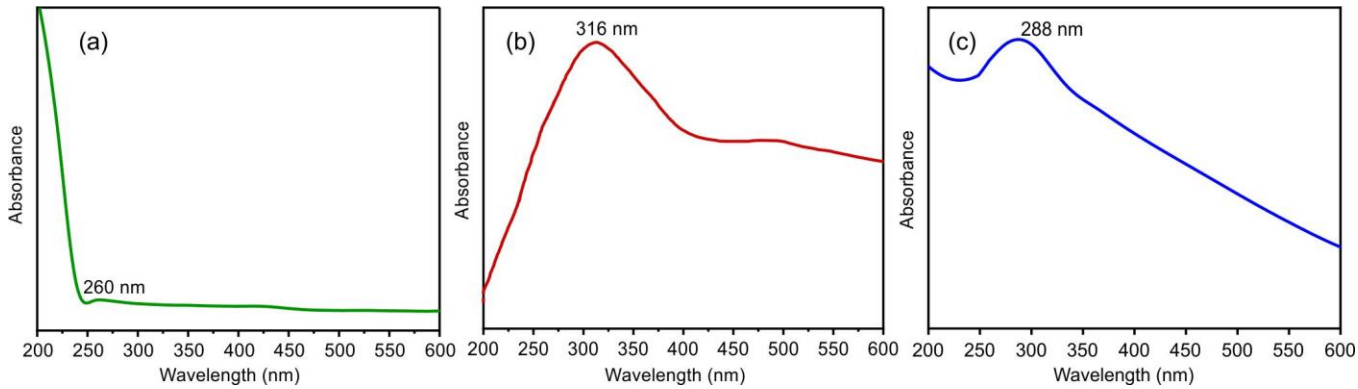

Fig. 1. UV-vis spectra of (a) DHA, (b) CNPs and (c) DHA@CSNPs

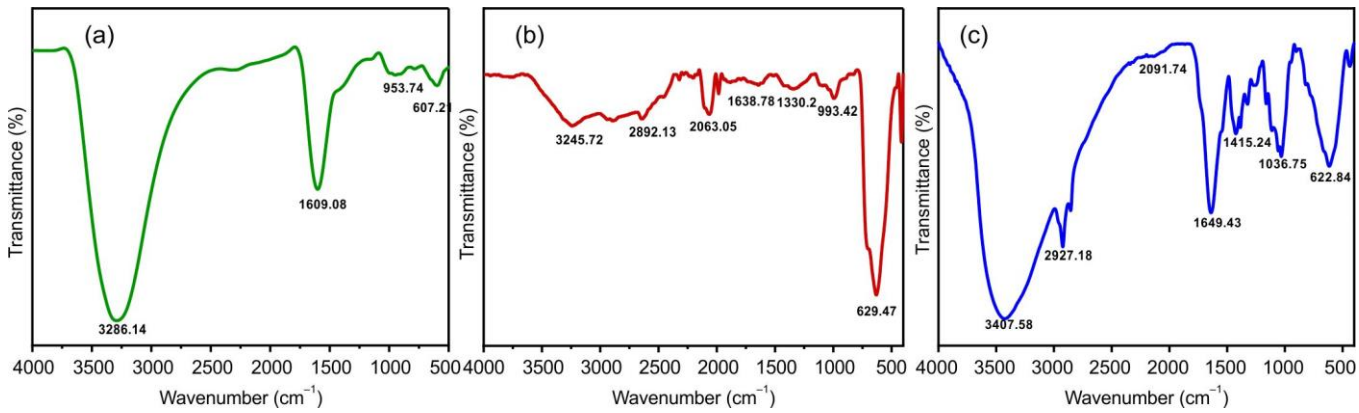

Fig. 2. FTIR spectra of (a) CNPs, (b) DHA and (c) DHA@CSNPs

groups [38], while the band at 1609.08 cm^{-1} is attributed to the amide-I (C=O stretching) of the chitosan backbone [38,39]. The peak at 953.74 cm^{-1} corresponds to C–O–C stretching of the polysaccharide linkage and the band at 607.21 cm^{-1} represents C–H bending and skeletal vibrations of chitosan. DHA exhibited a broad O–H stretching peak at 3245.72 cm^{-1} from the carboxylic acid group, with C–H stretching of methylene groups observed at 2892.13 cm^{-1}. The C=C stretching of *cis*-alkenes appeared at 1638.78 cm^{-1}, while C–H bending and out-of-plane bending of the alkenes were noted at 1330.2 and 993.42 cm^{-1}, respectively. A weak band at 2063.05 cm^{-1} was assigned to overtone or combination vibrations and 629.47 cm^{-1} corresponds to skeletal vibrations of the hydrocarbon chain. Upon encapsulation of DHA@CSNPs, the O–H/N–H stretching shifted to 3407.58 cm^{-1}, indicating hydrogen bonding between DHA and chitosan, while C–H stretching appeared at 2927.18 cm^{-1} [40]. The C=C/amide-I region shifted to 1649.43 cm^{-1}, confirming interaction and successful loading of DHA [41]. The peaks at 1415.24, 1036.75 and 622.84 cm^{-1} corresponded to C–H/O–H bending, C–O–C stretching and skeletal vibrations, confirming the structural integrity of chitosan in the nanocomposite [38].

SEM and FE-SEM with EDX studies: The surface morphology of DHA@CSNPs was investigated using SEM and FE-SEM analysis. SEM micrographs (Fig. 3) revealed aggregated nanoparticles with rough surface morphology, confirming the formation of DHA@CSNP polymeric nanostructures. At higher magnifications in FE-SEM (Fig. 4a-b), it is revealed that the DHA@CSNPs existed as compact nanoscale aggregates with rough surface morphology. Particle size analysis of the FE-SEM micrographs showed that the DHA@ CSNPs had an average diameter of 76.53 ± 3.41 nm, suggesting a relatively uniform particle size. Surface roughness and particle aggregation are common characteristics of chitosan nanoparticle systems [37]. EDX analysis was subsequently carried out to confirm the elemental composition of the synthesised nanoparticles.

The EDX spectrum demonstrated the presence of carbon (46.78 ± 0.25 wt.%, 54.78 ± 0.12 at%), oxygen (44.62 ± 0.09 wt.%, 38.13 ± 0.13 at%), nitrogen (5.89 ± 0.05 wt.%, 5.25 ± 0.03 at%) and a trace amount of sodium (2.05 ± 0.06 wt.%, 1.21 ± 0.04 at%), corresponding to the chitosan matrix. The high proportion of carbon, oxygen and nitrogen confirmed the polysaccharide and amine backbone of chitosan, whereas the presence of sodium is attributed to the ionic crosslinking process. Similar elemental compositions, including carbon, oxygen, nitrogen and sodium, are commonly identified in EDX analyses of CNP. These findings validate the successful synthesis of DHA@CSNPs with characteristic nanoscale morphology, controlled particle size and expected elemental composition.

XRD studies: The XRD pattern of DHA@CSNPs exhibited a prominent diffraction peak at 2θ = 20.78º, corresponding to the characteristic crystalline region of chitosan (Fig. 5). The presence of this peak confirms that the nanoparticles retained the semi-crystalline nature of chitosan after encapsulation. The average crystallite size, calculated using the Scherrer equation, was 43.56 nm, confirming the formation

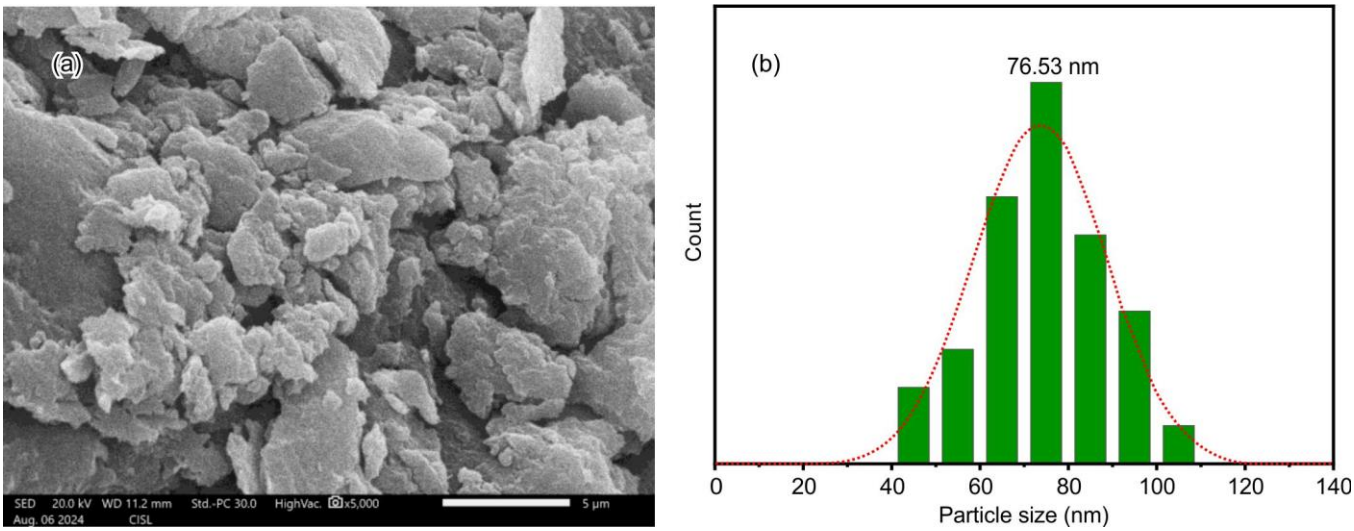

Fig. 3. (a) SEM image of DHA@CSNPs and (b) particle size distribution

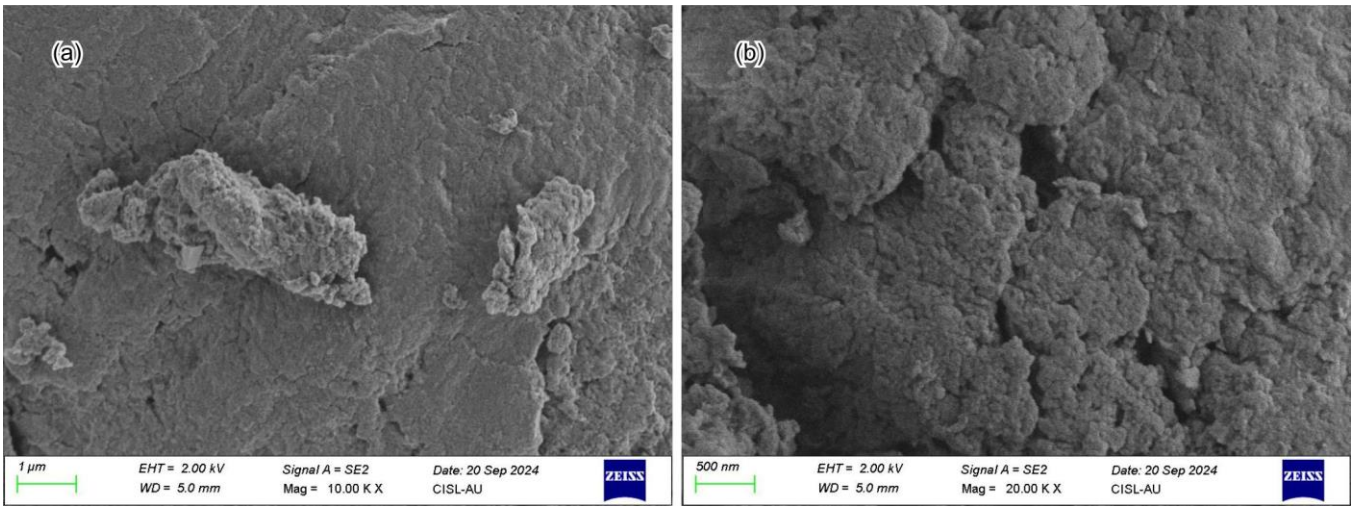

Fig. 4. FE-SEM micrographs (a) 1 µm and (b) 500 nm magnifications of DHA@CSNPs

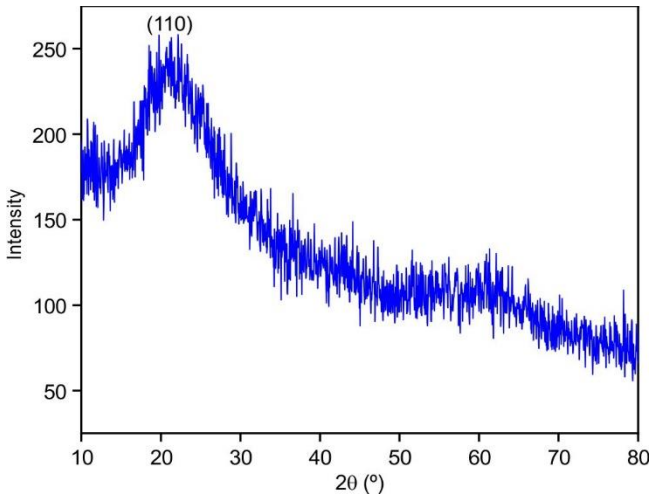

Fig. 5. XRD pattern of DHA@CSNPs

of nanoscale crystalline domains within the polymer matrix. Similar diffraction peaks at 2θ ≈ 20-21° have been reported for chitosan-based nanoparticles and are attributed to the crystalline structure of chitosan [37]. These results confirm the successful formation of DHA@CSNPs while preserving the structural characteristics of the chitosan matrix.

Zeta potential and DLS: The zeta potential of DHA@CSNPs was +21.63 mV (Fig. 6a), reflecting the presence of protonated amino groups on the chitosan surface. The positive surface charge promotes electrostatic repulsion between particles, thereby reducing aggregation and contributing to colloidal stability. Although zeta potential values exceeding ±25-30 mV are generally considered indicative of highly stable dispersions, values close to ±20 mV have also been reported to provide adequate stabilization through combined electrostatic and steric effects. Previous studies on chitosan nanoparticles have reported zeta potential values in the range of +21.8 to +26.3 mV, which are comparable to the value obtained in the present study [36].

DLS analysis revealed an average hydrodynamic diameter of 172.86 nm (Fig. 6b), confirming the formation of nanoparticles within the nanoscale range. The particle size distribution profile showed a single moderately broad peak, reflecting the presence of a major nanoparticle fraction. The

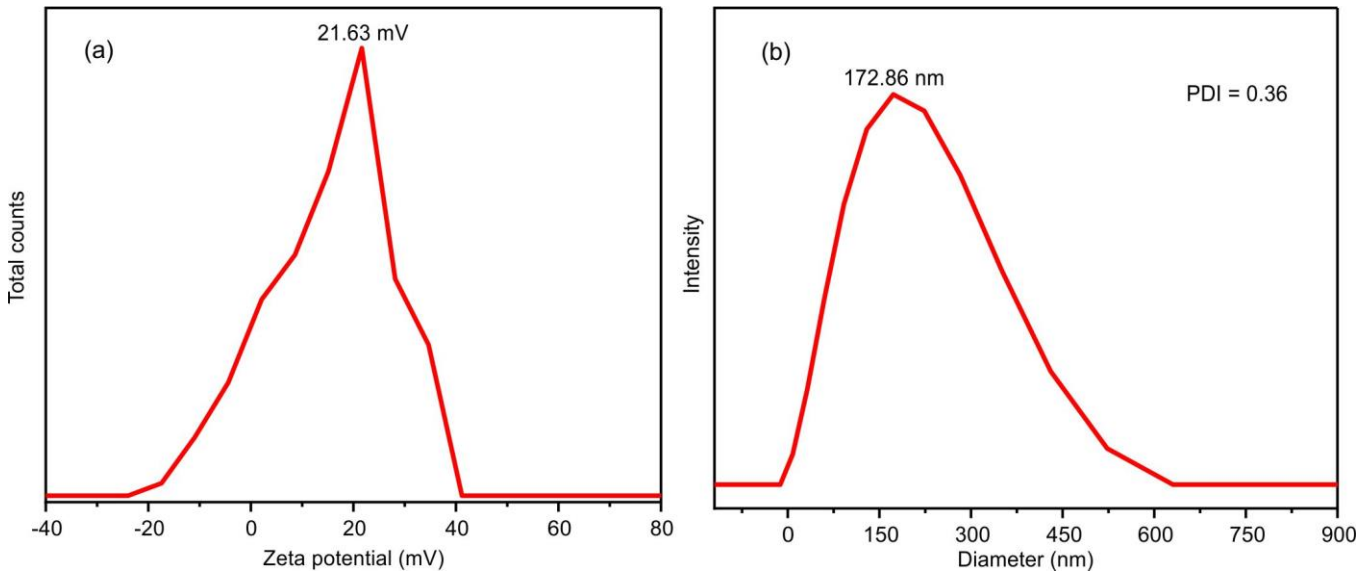

Fig. 6. (a) Zeta potential and (b) DLS spectrum of DHA@CSNPs

average hydrodynamic diameter of 172.86 nm falls within the size range considered suitable for cancer drug delivery, as nanoparticles smaller than 200 nm can prolong circulation and promote accumulation in tumour tissues through the enhanced permeability and retention (EPR) effect [42,43]. This particle size is comparable to those reported for chitosan-based nanocarriers developed for breast cancer treatment, which commonly range between 140 and 180 nm [44,45].

The PDI of DHA@CSNPs was 0.36, reflecting moderate variation in particle size. PDI values below 0.5 are generally considered acceptable for biomedical formulations, indicating a well-dispersed nanoparticle system [46,47]. The broader distribution relative to unloaded chitosan nanoparticles may arise from the incorporation of DHA, which can affect the ionic cross-linking between chitosan and tripolyphosphate during nanoparticle formation [44]. Taken together, the zeta potential, particle size and PDI measurements confirm the formation of a stable nanoscale formulation suitable for drug delivery applications.

Encapsulation efficiency (EE) and *in vitro* drug release: An EE of 83.38 ± 1.48% was achieved for DHA@CSNPs, reflecting the ability of the chitosan matrix to effectively retain DHA during nanoparticle formation (Fig. 7). This high encapsulation efficiency is comparable to or exceeds that reported for other drug-loaded chitosan nanoparticles, such as dihydroartemisinic-loaded chitosan nanoparticles showing 76.4% encapsulation efficiency. Encapsulation of ω-3 fatty acids, particularly DHA, within chitosan nanoparticles has been widely employed to minimize oxidative degradation and improve storage stability [48,49]. The *in vitro* release profile of DHA@CSNPs was investigated at pH 7.4 and pH 5.4 over a period of 24 h. The nanoparticles exhibited a marked pH-dependent release pattern, with DHA release being substantially greater under acidic conditions. After 24 h, the cumulative release reached 82.51% at pH 5.4, whereas only 17.76% of the encapsulated DHA was released at pH 7.4. The higher release at acidic pH can be attributed to the protonation of amino groups in chitosan, which promotes matrix hydration

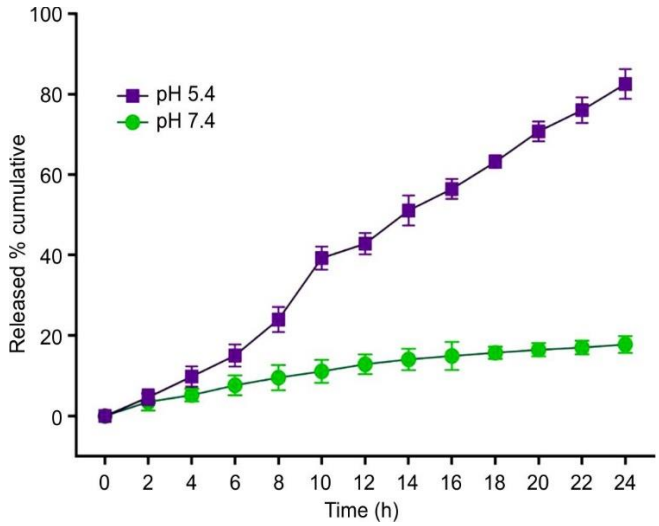

Fig. 7. *In vitro* drug release profiles of DHA@CSNPs at different pHs

and facilitates drug diffusion. Similar release behaviour has been reported for chitosan-based delivery systems and is associated with the pH-sensitive nature of the polymer. The observed release profile suggests that DHA@CSNPs can retain the payload under physiological conditions while promoting release in acidic environments, such as those found in tumour tissues and intracellular endosomal compartments.

Evaluation of antioxidant potential: DHA is a long-chain ω-3 PUFA containing six double bonds, a structure that makes it highly effective as a biological antioxidant but also extremely susceptible to oxidative degradation *via* autoxidation [50,51]. The chitosan matrix protects DHA from oxidative degradation while contributing additional antioxidant activity through its functional groups [51,52].

ABTS and DPPH radical scavenging: The ABTS and DPPH assays showed a concentration-dependent increase in radical scavenging activity for both free DHA and DHA@CSNPs (Figs. 8 and 9). At 50 μg/mL, DHA@CSNPs exhibited ABTS and DPPH scavenging activities of 60.38 ± 4.15%

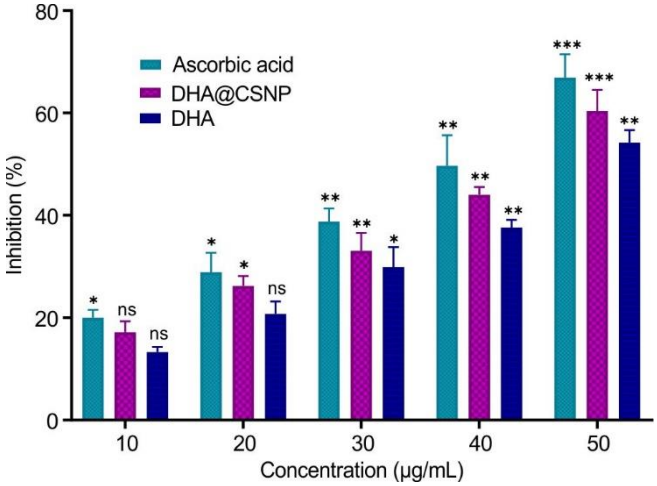

Fig. 8. ABTS radical scavenging activity. The values were expressed as the mean ± SD of triplicate experiments (n = 3) and the difference between the groups was evaluated by one-way ANOVA followed by Tukey's Post hoc test. *p < 0.05, **p < 0.01, ***p < 0.001 compared with ascorbic acid group

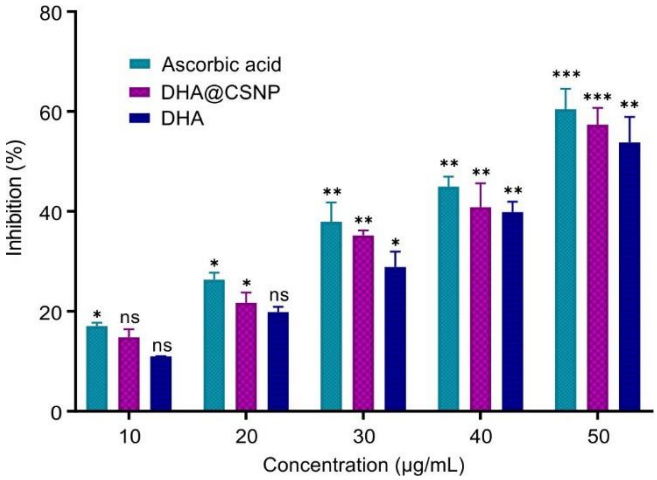

Fig. 9. DPPH radical scavenging activity. The values were expressed as the mean ± SD of triplicate experiments (n = 3) and the difference between the groups was evaluated by one-way ANOVA followed by Tukey's Post hoc test. *p < 0.05, **p < 0.01, ***p < 0.001 compared with ascorbic acid group

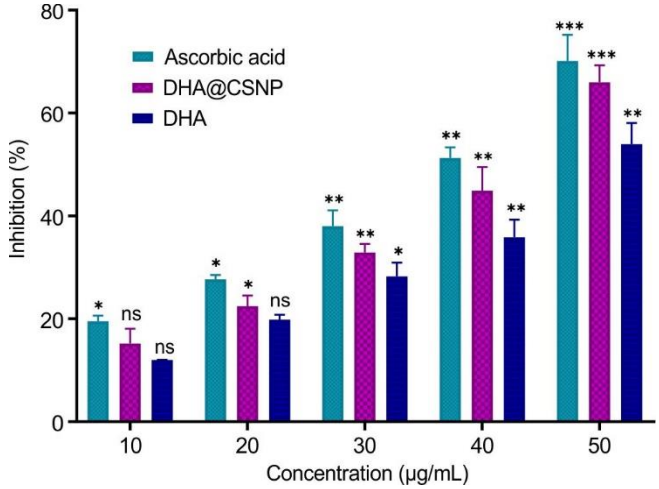

Fig. 10. Hydroxyl radical scavenging activity. The values were expressed as the mean ± SD of triplicate experiments (n = 3) and the difference between the groups was evaluated by one-way ANOVA followed by Tukey's Post hoc test. *p < 0.05, **p < 0.01, ***p < 0.001 compared with ascorbic acid group

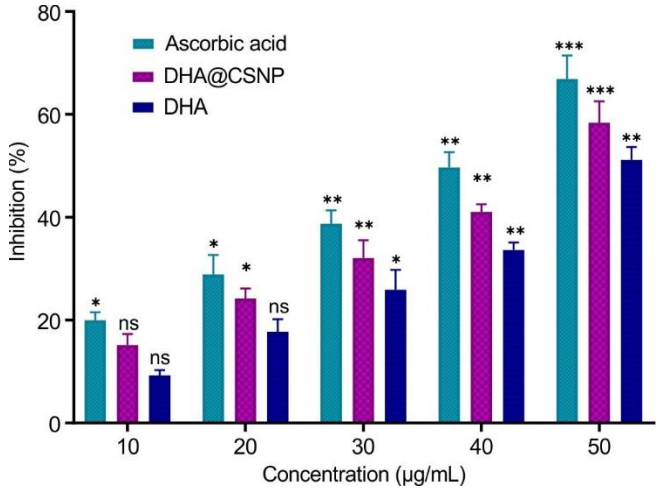

Fig. 11. Superoxide anion scavenging activity. The values were expressed as the mean ± SD of triplicate experiments (n = 3) and the difference between the groups was evaluated by one-way ANOVA followed by Tukey's Post hoc test. *p < 0.05, **p < 0.01, ***p < 0.001 compared with ascorbic acid group

and 57.38 ± 3.32%, respectively, which were higher than those observed for free DHA (54.18% and 53.82%, respectively).

The improved antioxidant activity of DHA@CSNPs was further supported by their lower IC_{50} values, with 42.88 µg/mL and 40.72 µg/mL recorded for the ABTS and DPPH assays, respectively, compared with 47.80 µg/mL and 45.30 µg/mL for free DHA. The enhanced radical scavenging activity may be attributed to the nanoscale nature of the formulation, which increases the available surface area for interaction with free radicals [53,54]. In addition, the amino and hydroxyl groups of chitosan can participate in radical quenching reactions, contributing to the antioxidant activity [55,56]. Similar improvements in antioxidant performance have been reported for other bioactive compounds encapsulated within chitosan nanoparticles [48,49].

Scavenging of hydroxyl and superoxide radicals: The scavenging activities against hydroxyl radicals (Fig. 10) and superoxide anions (Fig. 11) further demonstrated the improved antioxidant performance of DHA@CSNPs. The nanoformulation exhibited lower IC_{50} values for hydroxyl radicals (40.02 µg/mL) and superoxide anions (42.85 µg/mL) than free DHA (46.75 µg/mL and 47.60 µg/mL, respectively). The enhanced activity may be attributed to the protective effect of the chitosan matrix, which helps preserve DHA from oxidative degradation, together with the availability of reactive amino and hydroxyl groups on chitosan that participate in radical scavenging [56-59]. These findings suggest that DHA@CSNPs are more effective than free DHA in neutralising reactive oxygen species associated with oxidative stress [60].

Reducing power and nitric oxide (NO) scavenging: The reducing power assay (Fig. 12) measured the electron-donating ability of the compounds, showing an IC_{50} of 41.22 µg/mL for DHA@CSNPs. This enhancement over free DHA (46.50 µg/mL) highlights that the nano-environment preserves the

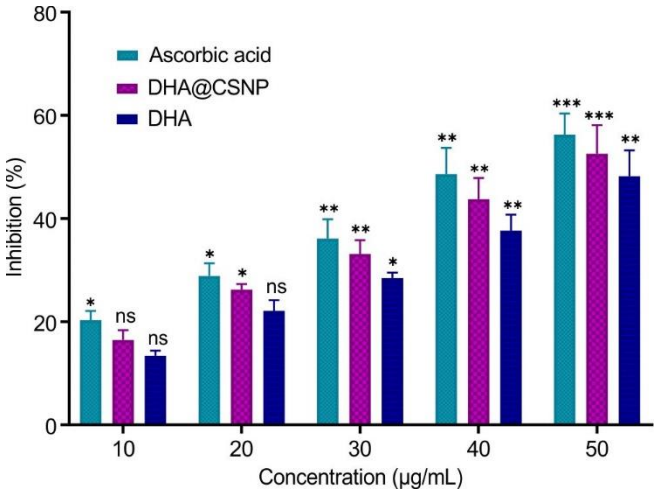

Fig. 12. Reducing powder activity. The values were expressed as the mean ± SD of triplicate experiments (n = 3) and the difference between the groups was evaluated by one-way ANOVA followed by Tukey's Post hoc test. *p < 0.05, **p < 0.01, ***p < 0.001 compared with ascorbic acid group

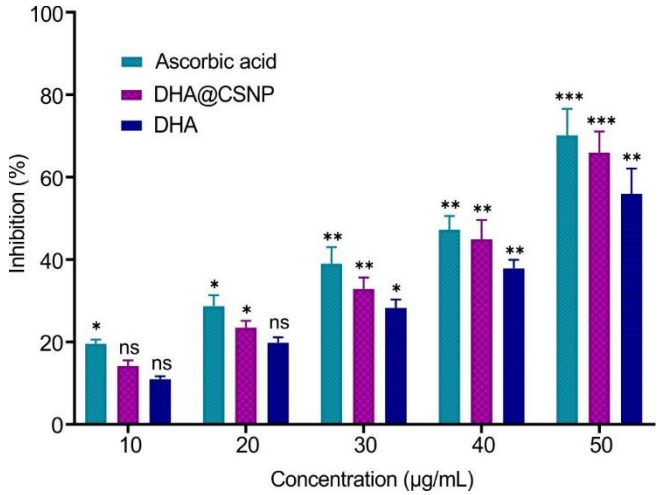

Fig. 13. Nitric acid activity. The values were expressed as the mean ± SD of triplicate experiments (n = 3) and the difference between the groups was evaluated by one-way ANOVA followed by Tukey's Post hoc test. *p < 0.05, **p < 0.01, ***p < 0.001 compared with ascorbic acid group

ability of DHA to terminate radical chain reactions by providing electrons [61,62]. Similarly, in the nitric oxide scavenging assay (Fig. 13), the nanoparticles achieved a high inhibition of 65.98 ± 5.09% at 50 µg/mL. Nitric oxide plays a complex role in inflammation and tumor progression; the ability of DHA@CSNPs to effectively scavenge NO suggests a potential role in conditions with prevalent nitrosative stress [63,64].

Cytotoxic potential against MDA-MB-231 breast cancer cells: The primary therapeutic efficacy of DHA@CSNPs was also evaluated against the MDA-MB-231 triple-negative breast cancer cell line. TNBC is characterised by its lack of estrogen, progesterone and HER2 receptors, making it particularly difficult to treat with conventional targeted therapies [65,66]. The MTT assay revealed a dose-dependent decrease in MDA-MB-231 cell viability, with an IC_{50} of 59.30 µg/mL (Fig. 14). This reflects a significant cytotoxic potential, especially considering that TNBC cells are often resistant to standard treatments [67]. Although chitosan is inherently biocompatible and exhibits low cytotoxicity, its primary function in this formulation is to enhance the solubility, stability and cellular delivery of DHA, thereby facilitating higher intracellular availability of the encapsulated compound [66,68]. Other research using chitosan to deliver anticancer agents such as 5-fluorouracil or hexahydro curcumin has shown that the nano-encapsulation strategy significantly lowers the dose required to achieve IC_{50} compared to the free drug [47,69].

Morphological analysis under phase-contrast microscopy provided visual confirmation of the cytotoxic effects. Cells treated with DHA@CSNPs exhibited hallmark signs of apoptosis such as cell shrinkage, rounding, membrane blebbing and cytoplasmic vacuolisation. In contrast, untreated control cells remained polygonal and densely packed [70,71]. These changes are indicative of the disruption of the cytoskeleton and the loss of cell membrane integrity, which are critical steps in programmed cell death [70]. Similar morphological shifts have been observed in breast cancer cells treated with other bioactive-loaded chitosan systems, confirming that the delivery vehicle does not interfere with the induction of apoptotic pathways [71,72]. The induction of apoptosis in cancer cells by DHA is a complex process involving multiple signalling pathways. Unlike its antioxidant role in normal

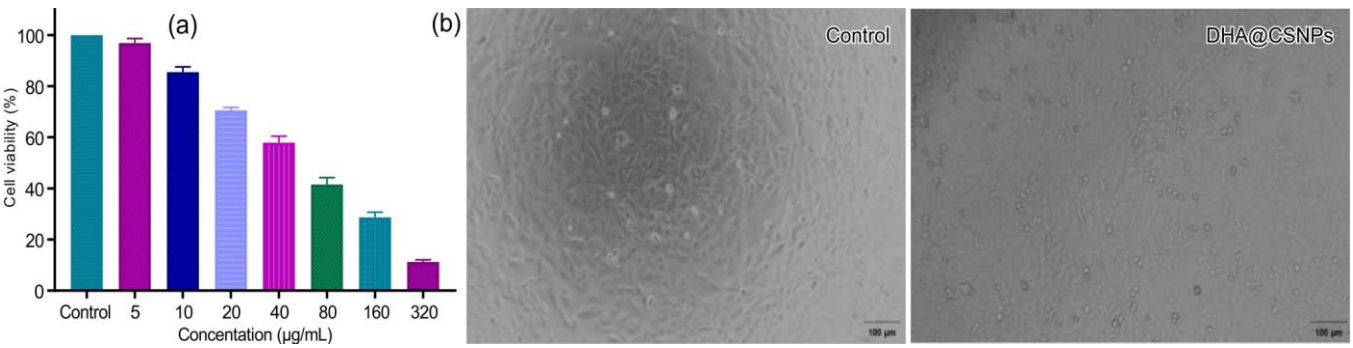

Fig. 14. MTT assay and morphological changes of MDA-MB-231 breast cancer cells treated with DHA@CSNPs. (a) Cell viability was determined using the MTT assay at various DHA@CSNPs concentrations (5-320 µg/mL). The data show a dose-dependent decrease in MDA-MB-231 cell viability, with an IC_{50} value of 59.30 µg/mL. (b) Representative images of A549 cells treated with DHA@CSNPs and the control. Cells treated with DHA@CSNPs display significant morphological changes, including cell shrinkage and detachment, compared to the control group. Scale bar = 100 µm

cells, DHA can act as a pro-oxidant in the specific environment of cancer cells. Upon uptake, DHA is incorporated into the cell membranes, where its high degree of unsaturation makes it a prime target for lipid peroxidation [67,72]. In MDA-MB-231 cells, the accumulation of lipid hydroperoxides and the subsequent increase in intracellular ROS trigger the mitochondrial apoptotic pathway [67].

Conclusion

This study demonstrates that chitosan-based nanoparticles efficiently encapsulate DHA, enhancing its physicochemical stability, antioxidant activity and anticancer potential. DHA @CSNPs exhibited uniform nanoscale morphology, a semi-crystalline structure and favourable colloidal stability, enabling sustained, pH-responsive release that preferentially occurs under acidic conditions, similar to those in tumor microenvironments. Antioxidant assays confirmed that nano-encapsulation significantly improved radical-scavenging activity against ABTS, DPPH, hydroxyl, superoxide and nitric oxide species, surpassing that of free DHA. *In vitro* cytotoxic evaluation against MDA-MB-231 breast cancer cells revealed dose-dependent apoptosis with an IC_{50} of 59.30 μg/mL, indicating potent therapeutic efficacy. The ability of DHA@CSNPs to improve DHA stability and intracellular delivery contributed to enhanced antioxidant and anticancer activities. These results demonstrate the potential of DHA@CSNPs as a nanodelivery platform and provide a basis for future *in vivo* investigations.

CONFLICT OF INTEREST

The authors declare that there is no conflict of interests regarding the publication of this article.

DECLARATION OF AI-ASSISTED TECHNOLOGIES

During the preparation of this manuscript, the authors used an AI-assisted tool(s) to improve the language. The authors reviewed and edited the content and take full responsibility for the published work.

REFERENCES

1. D. Swanson, R. Block and S. A. Mousa, *Adv. Nutr.*, **3**, 1 (2012); https://doi.org/10.3945/an.111.000893
2. S.M. Borgonovi, S. Iametti and M. Di Nunzio, *Antioxidants*, **12**, 1283 (2023); https://doi.org/10.3390/antiox12061283
3. J. Li, B.L.R. Pora, K. Dong and J. Hasjim, *Food Sci. Nutr.*, **9**, 5229 (2021); https://doi.org/10.1002/fsn3.2299
4. L.A. Horrocks and K.Y. Young, *Pharmacol. Res.*, **40**, 211 (1999); https://doi.org/10.1006/phrs.1999.0495
5. S. Wu, H. Peng, S. Li, L. Huang, X. Wang, Y. Li, Y. Liu, P. Xiong, Q. Yang, K. Tian, W. Wu, R. Pu, X. Lu, Z. Xiao, J. Yang, Z. Zhong, Y. Gao, Y. Deng, and Y. Deng, *Cancer Immunol. Res.*, **12**, 744 (2024); https://doi.org/10.1158/2326-6066.CIR-23-0359
6. I. Djuricic and P.C. Calder, *Curr. Atheroscler. Rep.*, **27**, 116 (2025); https://doi.org/10.1007/s11883-025-01363-2
7. W. Guo, X. Ge, J. Lu, X. Xu, J. Gao, Q. Wang, C. Song, Q. Zhang and C. Yu, *Nutrients*, **14**, 5335 (2022); https://doi.org/10.3390/nu14245335
8. A. Michalak, P. Mosińska and J. Fichna, *Front. Pharmacol.*, **7**, 459 (2016); https://doi.org/10.3389/fphar.2016.00459
9. C.H.S. Ruxton, P.C. Calder, S.C. Reed and M.J. Simpson, *Nutr. Res. Rev.*, **18**, 113 (2005); https://doi.org/10.1079/NRR200497
10. J. Bradbury, *Nutrients*, **3**, 529 (2011); https://doi.org/10.3390/nu3050529
11. G.C. Burdge and P.C. Calder, *Reprod. Nutr. Dev.*, **45**, 581 (2005); https://doi.org/10.1051/rnd:2005047
12. Y. Lin, J.R. Hibbeln, A.F. Domenichiello, C.E. Ramsden, N.M. Salem, C.T. Chen, H. Jin, A.B. Courville, S.F. Majchrzak-Hong, S.I. Rapoport, R.P. Bazinet and B.V. Miller III, *Lipids*, **53**, 535 (2018); https://doi.org/10.1002/lipd.12055
13. W. Lv and D. Xu, *Foods*, **11**, 2685 (2022); https://doi.org/10.3390/foods11172685
14. H. Singh, C.B.M. Kumar, N. Singh, S. Paul and S.K. Jain, *Food Funct.*, **9**, 2213 (2018); https://doi.org/10.1039/C7FO01391D
15. J. Wang, J. Ossemond, J. Jardin, V. Briard-Bion, G. Henry, Y. Le Gouar, O. Ménard, S. Lê, A. Madadlou, D. Dupont and F. Pédrono, *Food Res. Int.*, **162B**, 112112 (2022); https://doi.org/10.1016/j.foodres.2022.112112
16. M. Chidambaram, R. Manavalan and K. Kathiresan, *J. Pharm. Pharm. Sci.*, **14**, 67 (2011); https://doi.org/10.18433/J30C7D
17. R. Singh, A. Sharma, J. Saji, A. Umapathi, S. Kumar and H.K. Daima, *Nano Converg.*, **9**, 21 (2022); https://doi.org/10.1186/s40580-022-00313-x
18. J.P. Quiñones, H. Peniche and C. Péniche, *Polymers*, **10**, 235 (2018); https://doi.org/10.3390/polym10030235
19. M.A. Mohammed, J.T. Syeda and K.M. Wasan, *Pharmaceutics*, **9**, 53 (2017); https://doi.org/10.3390/pharmaceutics9040053
20. Y. Qin, C. Qian, W. Li, Q. Wang, Q. Sheng, Z. Chen, W. Zhang, W. Li, G. Ge, Z. Yan and D. Geng, MedComm, **7**, e70600 (2026); https://doi.org/10.1002/mco2.70600
21. C. Andrés, J.M.P. Lastra, F.J. Plou and E. Perez-Lebena, *Int. J. Mol. Sci.*, **22**, 4642 (2021); https://doi.org/10.3390/ijms22094642
22. V. Cecarini, J. Gee, E. Fioretti, M. Amici, M. Angeletti, A.M. Eleuteri and J.N. Keller, *Biochim. Biophys. Acta Mol. Cell Res.*, **1773**, 93 (2007); https://doi.org/10.1016/j.bbamcr.2006.08.039
23. A. Ozcan and M. Ogun, in eds.: S.J.T. Gowder, Biochemistry of Reactive Oxygen and Nitrogen Species, In: Basic Principles and Clinical Significance of Oxidative Stress, InTech, Chap. 3, pp. 37–58 (2015); https://doi.org/10.5772/61193
24. G. Gloire, S. Legrand-Poels and J. Piette, *Biochem. Pharmacol.*, **72**, 1493 (2006); https://doi.org/10.1016/j.bcp.2006.04.011
25. A.A. Elzatahry and M.M. Eldin, *Polym. Adv. Technol.*, **19**, 1787 (2008); https://doi.org/10.1002/pat.1195
26. N.A. Emad, Y. Sultana, M. Aqil, A. Saleh and F.A. Nasr, *Saudi J. Biol. Sci.*, **30**, 103778 (2023); https://doi.org/10.1016/j.sjbs.2023.103778
27. J.S. Hussein, W. Rasheed, T. Ramzy, M. Nabeeh, M. Harvy, S. El-Toukhy, O. Ali, J. Raafat and M. El-Naggar, *Hum. Exp. Toxicol.*, **38**, 962 (2019); https://doi.org/10.1177/0960327119843586
28. R. Re, N. Pellegrini, A. Proteggente, A. Pannala, M. Yang and C. Rice-Evans, *Free Rad. Biol. Med.*, **26**, 1231 (1999); https://doi.org/10.1016/S0891-5849(98)00315-3
29. Z. Yan, X. Wang, P. Zhao, Y. He, X. Meng, and B. Liu, *Food Chem.*, **441**, 138289 (2024); https://doi.org/10.1016/j.foodchem.2023.138289
30. A.H. Ali, M. Hachem and M.K. Ahmmed, *Heliyon*, **10**, e30946 (2024); https://doi.org/10.1016/j.heliyon.2024.e30946
31. C. Xu, L. Shu, L. Zhiqiang, S. Fengrui and L. Shuying, *Anal. Chim. Acta*, **793**, 53 (2013); https://doi.org/10.1016/j.aca.2013.07.027
32. G.C. Yen and H.Y. Chen, *J. Agric. Food Chem.*, **43**, 27 (1995); https://doi.org/10.1021/jf00049a007
33. L. Marcocci, J. J. Maguire, M. T. Droy-Lefaix and L. Packer, *Biochem. Biophys. Res. Commun.*, **201**, 748 (1994); https://doi.org/10.1006/bbrc.1994.1764
34. J.G.J. Almukhtar and F.F. Karam, *J. Phys. Conf. Ser.*, **1664**, 012071 (2020); https://doi.org/10.1088/1742-6596/1664/1/012071

35. V. Arulmozhi, K. Pandian and S. Mirunalini, *Colloids Surf. B Biointerfaces*, **110**, 313 (2013); https://doi.org/10.1016/j.colsurfb.2013.03.039
36. N.E. El-Naggar, M. Eltarahony, E.S.E. Hafez and S.I. Bashir, *Sci. Rep.*, **13**, 11127 (2023); https://doi.org/10.1038/s41598-023-37660-6
37. N.E. El-Naggar, A.M. Shiha, H. Mahrous and A.B.A. Mohammed, *Sci. Rep.*, **14**, 11336 (2024); https://doi.org/10.1038/s41598-024-59702-3
38. I. Corazzari, R. Nisticò, F. Turci, M.G. Faga, F. Franzoso and S. Tabasso, *Polym. Degrad. Stab.*, **112**, 1 (2015); https://doi.org/10.1016/j.polymdegradstab.2014.12.006
39. C.P. Kiilll, H. Barud, S. Santagneli, S.H. Ribeiro, S.J.L. Ribeiro, A.M. Silva, A. Tercjak, J. Gutierrez, A.M. Pironi and M.P.D. Gremião, *Carbohydr. Polym.*, **157**, 1695 (2016); https://doi.org/10.1016/j.carbpol.2016.11.053
40. S. Khoshnood, B. Negahdari, V. Kaviar, V.H. Sadeghifard, M.A. Abdullah, M.B. Elshazly and M.H. Haddadi, *Front. Microbiol.*, **14**, 1083330 (2023); https://doi.org/10.3389/fmicb.2023.1083330
41. H. Yang, P. Wen, K. Feng, M.H. Zong, W.Y. Lou and H. Wu, *RSC Adv.*, **7**, 14939 (2017); https://doi.org/10.1039/C7RA00051K
42. P. Patil and S.G. Killedar, *J. Drug Deliv. Sci. Technol.*, **63**, 102523 (2021); https://doi.org/10.1016/j.jddst.2021.102523
43. R. Thagele, A. Bagre and M.L. Kori, *J. Drug Deliv. Ther.*, **9**, 1 (2019); https://doi.org/10.22270/jddt.v9i1.2151
44. M.J. Masarudin, S.M. Cutts, B.J. Evison, D.R. Phillips and P.J. Pigram, *Nanotechnol. Sci. Appl.*, **8**, 67 (2015); https://doi.org/10.2147/NSA.S91785
45. F.A. Taher, W. Moselhy, A.F. Mohamed, E.E.D. Samia, M.M. Karima and A.B. Zayed, *Int. J. Adv. Res.*, **5**, 370 (2017); https://doi.org/10.21474/IJAR01/4122
46. R.A. Bashirah, N.B. Zamri, N.B. Alitheen, S. Ismail and M.J. Masarudin, *Naunyn Schmiedebergs Arch. Pharmacol.*, **399**, 2969 (2026); https://doi.org/10.1007/s00210-025-04592-z
47. S. Anjum, F. Naseer, T. Ahmad, F. Jahan, H. Qadir, R. Gul, K. Kousar, A. Sarwar and A. Shabbir, *Sci. Rep.*, **14**, 11431 (2024); https://doi.org/10.1038/s41598-024-55900
48. N.L.V. Braber, A.J. Paredes, Y. Rossi, C. Porporatto, D.A. Allemandi, C.D. Borsarelli, S.G. Correa, and M.A. Montenegro, *Int. J. Biol. Macromol.*, **112**, 399 (2018); https://doi.org/10.1016/j.ijbiomac.2018.01.085
49. E.S. Kim, Y. Baek, H.J. Yoo and J.S. Lee, *Antioxidants*, **11**, 479 (2022); https://doi.org/10.3390/antiox11030479
50. P.K. Chang, M. Tsai, C.Y. Huang, C. Lee, C. Lin, C. Shieh and C.-H. Kuo, *Mar. Drugs*, **19**, 470 (2021); https://doi.org/10.3390/md19080470
51. Z. Shen, M.A. Augustin, L. Sanguansri and C. Li, *J. Agric. Food Chem.*, **58**, 4487 (2010); https://doi.org/10.1021/jf904102k
52. S. Gulzar, N. Raju, T. Prodpran and S. Benjakul, *Eur. J. Lipid Sci. Technol.*, **124**, 2100178 (2022); https://doi.org/10.1002/ejlt.202100178
53. F. Teymouri and E. Karimi, *Discov. Oncol.*, **15**, 100 (2024); https://doi.org/10.1007/s12672-024-00957-7
54. M. Almukainzi, T. A. El-Masry, E.I. El-Zahaby and M.M.F. El-Nagar, *Pharmaceuticals*, **17**, 999 (2024); https://doi.org/10.3390/ph17080999
55. X. Zhai, C. Zhang, G. Zhao, S. Stoll, F. Ren and X. Leng, *J. Nanobiotechnol.*, **15**, 4 (2017); https://doi.org/10.1186/s12951-016-0243-4
56. Y. Jampafuang, A. Tongta and Y. Waiprib, *Polymers*, **11**, 2010 (2019); https://doi.org/10.3390/polym11122010
57. P. Sacco, E. Decleva, F. Tentor, R. Menegazzi, M. Borgogna, S. Paoletti, K.A. Kristiansen, K.M. Vårum and E. Marsich, *Macromol. Biosci.*, **17**, 1700214 (2017); https://doi.org/10.1002/mabi.201700214
58. S.A. Mubeena and R. Preetha, *Sustain. Food Technol.*, **4**, 930 (2026); https://doi.org/10.1039/D5FB00388A
59. Z. Wang, Y. Yan, Z. Zhang, C. Li, L. Mei, R. Hou, X. Liu and H. Jiang, *Polymers*, **16**, 867 (2024); https://doi.org/10.3390/polym16070867
60. F. Luan, L. Wei, J. Zhang, Y. Mi, F. Dong, Q Li and Z. Guo, *Polymers*, **10**, 395 (2018); https://doi.org/10.3390/polym10040395
61. E. Galani, I. Ly, É. Laurichesse, G. Zoumpopoulou, E. Tsakalidou, V. Schmitt, A. Xenakis and M.D. Chatzidaki, *Colloids Surf. A Physicochem. Eng. Asp.*, **683**, 133002 (2023); https://doi.org/10.1016/j.colsurfa.2023.133002
62. L.S. Simões, D.A. Madalena, A.C. Pinheiro, J.A. Teixeira, A.A. Vicente and Ó.L. Ramos, *Adv. Colloid Interface Sci.*, **243**, 23 (2017); https://doi.org/10.1016/j.cis.2017.02.010
63. C. Gómez-Gaete, J. Avendaño-Godoy, D. Escobar-Avello, V.H. Campos-Requena, C. Rogel-Castillo, L.M. Estevinho, M. Martorell, J. Sharifi-Rad and D. Calina, *Food Prod. Process. Nutr.*, **6**, 8 (2024); https://doi.org/10.1186/s43014-023-00190-9
64. F. Salehi, H. Behboudi, G. Kavoosi and S.K. Ardestani, *RSC Adv.*, **7**, 43141 (2017); https://doi.org/10.1039/C7RA06793C
65. S.A. Abdulmalek, A.M. Saleh, Y.R. Shahin and E.F. El-Azab, *Naunyn Schmiedebergs Arch. Pharmacol.*, **397**, 6941 (2024); https://doi.org/10.1007/s00210-024-03068-w
66. P. Bougnoux, N. Hajjaji, M.N. Ferrasson, B. Giraudeau, C. Couet and O.L. Floch, *Br. J. Cancer*, **101**, 1978 (2009); https://doi.org/10.1038/sj.bjc.6605441
67. S.A. Loutfy, H.M.A. El-Din, M.H. Elberry, N.G. Allam, M. Taha and A. Abdellah, *Adv. Nat. Sci. Nanosci. Nanotechnol.*, **7**, 035008 (2016); https://doi.org/10.1088/2043-6262/7/3/035008
68. F.N. Sorasitthiyanukarn, C. Muangnoi, C.B. Gomez, A. Suksamrarn and P. Rojsitthisak, *Pharmaceutics*, **15**, 472 (2023); https://doi.org/10.3390/pharmaceutics15020472
69. C.A.F. Ghaly, A. Bakaar and A.F. Mohamed, *J. Egypt. Soc. Parasitol.*, **48**, 379 (2018); https://doi.org/10.12816/0050445
70. A.M.H. Al-Rajhi and T.M.A. Ghany, *Appl. Biol. Chem.*, **66**, 33 (2023); https://doi.org/10.1186/s13765-023-00788-0
71. I.N.A.A. Al-Fatlawi, V. Pouresmaeil, F. Davoodi-Dehaghani and A. Pouresmaeil, *BMC Biotechnol.*, **24**, 18 (2024); https://doi.org/10.1186/s12896-024-00845-6
72. E. Germain, V. Chajès, S. Cognault, C. Lhuillery and P. Bougnoux, *Int. J. Cancer*, **75**, 578 (1998); https://doi.org/10.1002/(SICI)1097-0215(19980209)75:4<578::AID-IJC14>3.0.CO;2-5